AIAA JOURNAL
Vol. 43, No. 12, December 2005

Shear Lag Micromechanics Model for Effective Properties of Piezoelectric Composites

Nilanjan Mallik*
Banaras Hindu University, Varanasi 221 005, India

Prediction of the effective properties of piezoelectric composites with the help of shear lag micromechanics model is discussed. The shear lag micromechanics model is derived by considering a representative volume of the composite that contains a piezoelectric inclusion. Both homogeneous and heterogeneous inclusion problems are considered. In the homogeneous inclusion problem, a piezoelectric inclusion is present inside a piezoelectric medium, whereas in heterogeneous inclusion either a piezoelectric inclusion is present inside a matrix medium or a matrix inclusion is present inside a piezoelectric medium. A new matrix method is followed for evaluation of effective properties of the piezoelectric composite using a shear lag model. The inclusion considered is of rectangular parallelopiped type. The effect of the geometry of the inclusion on the effective mechanical and piezoelectric properties of the composite is studied.

Nomenclature

b = width
C = matrix of stiffness coefficient
$\boldsymbol{D}$ = dielectric displacement vector
$\boldsymbol{E}$ = electric field vector
$\boldsymbol{e}$ = piezoelectric stress coefficient vector
f = volume fraction
ℓ = length
s = applied strain
t = thickness
$\boldsymbol{U}$ = displacement vector
u = displacement component along x direction
v = displacement component along y direction
w = displacement component along z direction
γ = shear strain
ε = dielectric matrix
ϵ = strain tensor
σ = stress tensor
$\boldsymbol{\tau}$ = shear stress vector

Superscripts

c = composite
ic = inclusion
m = matrix

I. Introduction

OF late applications such as structural vibration damping, acoustical control of flexible structures, underwater transducers, and medical imaging utilize piezoelectric materials both in monolithic and composite form. The main drawback of the existing monolithic piezoelectric materials is that the control authority of these materials is very low because their piezoelectric stress/strain coefficients are of very small magnitudes. Because the active damping of smart structures depends on the magnitude of the piezoelectric coefficients, tailoring of these properties can improve the damping characteristics of lightweight smart structures. Research on piezoelectric composites has come through micromechanical estimates of their mechanical and electromechanical properties. Aboudi[1] carried out a micromechanical analysis to predict the effective coefficients of piezoelectric fiber-reinforced composites considering different electric fields in the fibers and matrix, which are related to average composite electric field. He used the method of cells for deriving the effective properties of the piezoelectric composites. His prediction for the piezoelectric constant, which gives rise to actuation in the fiber direction, does not show improvement over that of the piezoelectric material alone. The research of Smith and Auld[2] is for 1-3 piezoelectric composites. Their composites are constructed such that the rods of piezoelectric materials are embedded vertically, that is, aligned along the thickness of the composite, in a polymer base matrix such that the electric fields are applied along the length of the piezoelectric fibers. The strength of material approach was used for predicting the effective properties. These composites show marginal improvement of the effective piezoelectric constant of the piezocomposite, which quantifies the deformations in the fiber direction.

Dunn and Taya[3] evaluated the effective properties of multiphase composites through dilute, self-consistence and Mori–Tanaka approximations. Recently, Mallik and Ray[4] derived the effective properties of piezoelectric fiber-reinforced composites (PFRC) with the help of two micromechanics methods, namely, strength of materials approach and method of cells. The constructional feature of PFRC is that the piezoelectric fibers are oriented longitudinally in the matrix and the electric field is applied in the direction transverse to the fiber direction. The study predicted improved piezoelectric properties to a transverse direction to that of the applied electric field. Mallik[5] investigated effective properties of piezoelectric composites in a plane stress situation. The effective properties of a short fiber inclusion problem are derived through the Eshelby[6] tensor method. The shear lag model for the piezoelectric inclusion problem was originally developed by Cox,[7] and its detailed derivation is summarized by Kelly.[8] A good account of the procedure is also available by Taya and Arsenault.[9] The procedure is best suited for an aligned short-fiber composite, where short fibers of uniform length and diameter (hence constant aspect ratio) are all aligned in the loading direction and distributed uniformly throughout the material. References 10–13 can be mentioned here in the field of micromechanics estimates of the piezoelectric composites. The equivalent inclusion method is applied to study the work hardening behavior of piezoelectric composites by Huang.[11] Effective properties of platelet-reinforced piezocomposites were investigated by Chen.[14] The finite element method was also applied to model debonding in the fiber matrix interface, and hence, effective properties were derived.[15] The majority of the literature available for determining effective behavior of piezoelectric inclusion follows either the Eshelby tensor approach or

Received 27 February 2005; revision received 12 May 2005; accepted for publication 12 May 2005.

*Lecturer, Department of Mechanical Engineering, Institute of Technology; get_nilu@yahoo.com.

finite element method. However, no literature is currently available for the shear lag micromechanics model for piezoelectric composites even though it is very simple. Thus, the need for investigation on the modeling of piezoelectric inclusion problem using the shear lag method is established.

Hence, this paper is devoted to theoretical investigations on the prediction of effective properties of pizoelectric composites using the shear lag model. The effect of the inclusion geometry on the effective mechanical and piezoelectric properties is considered for investigation. The shape of the inclusion considered is that of a rectangular parallelopiped. A new matrix method is presented for the derivation of effective properties of piezoelectric composites.

II. Shear Lag Model

Figure 1 shows a transverse cross section of a representative short-fiber composite. It is assumed that the bond between the fibers and the matrix is perfect, the composite is homogeneous, and the fibers are continuous and parallel. The inclusions are oriented in a preferred direction, namely, longitudinally, that is, along the x axis. Also the fiber and matrix materials are considered to be linearly elastic. For the homogeneous inclusion problem, the fibers, that is, the inclusions and matrix, are made of piezoelectric material, and for heterogeneous inclusion problem, either of the two phases is a piezoelectric medium. For the heterogeneous inclusion problem, the matrix medium is piezoelectrically inactive. In general, the micromechanical analysis is confined to a representative volume that includes both fiber and the surrounding matrix. The unit cell, which is a representative short-fiber surrounded by the matrix, is shown in Fig. 2. The length, width, and thickness of this representative unit cell of the composite are denoted by ℓ^c, b^c, and t^c, respectively, whereas ℓ^{ic}, b^{ic}, and t^{ic} are the length, width, and thickness of the short-fiber inclusion occupied in the unit cell, respectively.

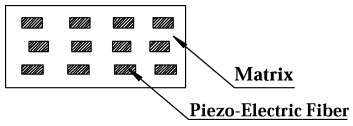

Fig. 1 Longitudinal cross section of piezoelectric short-fiber composite.

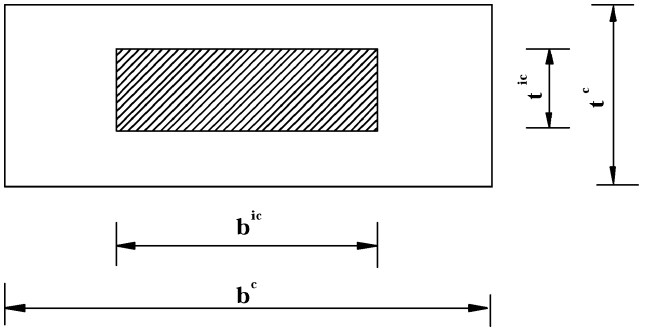

Fig. 2a Transverse cross section of representative volume element of piezoelectric short-fiber composite.

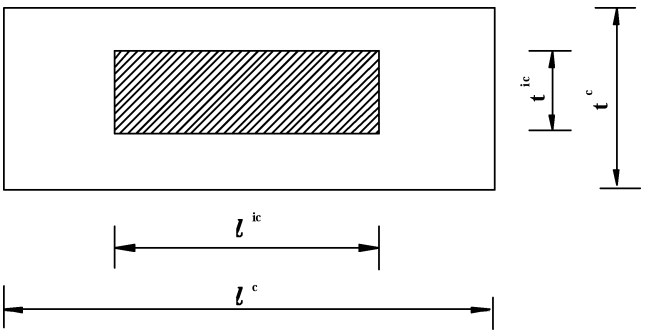

Fig. 2b Longitudinal cross section of representative volume element of piezoelectric short-fiber composite.

The other boundary of the surrounding matrix is taken as the midsurface between two short fibers. Let this aligned short-fiber composite be subjected to the applied normal strains s_x, s_y, and s_z along the x, y, and z directions, respectively. The constitutive relations for the material of the piezoelectric medium as given by Tiersten[16] are

$$\sigma_{ij} = C_{ijkl}\epsilon_{kl} - \boldsymbol{e}_{kij}\boldsymbol{E}_k \tag{1}$$

$$\boldsymbol{D}_i = \boldsymbol{e}_{ikl}\epsilon_{kl} + \varepsilon_{ik}\boldsymbol{E}_k \tag{2}$$

If matrix phase is piezoelectrically inactive, then its constitutive relation is given by

$$\sigma_{ij} = C_{ijkl}\epsilon_{kl} \tag{3}$$

$$\boldsymbol{D}_i = \varepsilon_{ik}\boldsymbol{E}_k \tag{4}$$

C and ε are the stiffness coefficient matrix, and dielectric constant matrix, respectively. It is assumed that the electric field applied in the z direction of the composite does not produce any field in the other two orthogonal directions.

The constitutive relations, keeping out the shear stress terms for the material of the inclusion if it is piezoelectric medium, can be written as

$$\{\sigma\}^{ic} = [C]^{ic}\{\epsilon\}^{ic} - \{e\}^{ic}\boldsymbol{E}_z^{ic} \tag{5}$$

where

$$\{\sigma\}^{ic} = \{\sigma_x \quad \sigma_y \quad \sigma_z\}^{ic}, \qquad \{\epsilon\}^{ic} = \{\epsilon_x \quad \epsilon_y \quad \epsilon_z\}^{ic}$$

$$\{e\}^{ic} = \{e_{31} \quad e_{32} \quad e_{33}\}^{ic}, \qquad [C]^{ic} = \begin{bmatrix} C_{11} & C_{12} & C_{13} \\ C_{21} & C_{22} & C_{23} \\ C_{31} & C_{32} & C_{33} \end{bmatrix}^{ic}$$

In which σ_x, σ_y, and σ_z are the normal stresses in the x, y, and z directions, respectively; ϵ_x, ϵ_y, and ϵ_z are the corresponding normal strains; C_{ij}, $i, j = 1, 2, \ldots, 6$, are the elastic constants; e_{31}, e_{32}, and e_{33} are the piezoelectric stress coefficients; $\boldsymbol{E}_z^{ic}$ is the electric field component in the z direction, that is, across the thickness of the inclusion. Note that the piezoelectric constants e_{31}, e_{32}, and e_{33} are the measure of induced normal stresses in the x, y, and z directions, respectively, due to the applied unit electric field in the z direction.

When strain–displacement relations are used, Eq. (5) can be rewritten as

$$[C]^{ic}\left\{\frac{\partial U}{\partial x}\right\}^{ic} = \{\sigma\}^{ic} + \{e\}^{ic}\boldsymbol{E}_z^{ic} \tag{6}$$

where

$$\left\{\frac{\partial U}{\partial x}\right\}^{ic} = \left\{\frac{\partial u}{\partial x} \quad \frac{\partial v}{\partial y} \quad \frac{\partial w}{\partial z}\right\}^{ic}$$

in which u, v, and w are the displacements along the x, y, and z directions, respectively.

The solution of $\{\partial U/\partial x\}^{ic}$ can be obtained from Eq. (6) as

$$\left\{\frac{\partial U}{\partial x}\right\}^{ic} = \frac{1}{\xi}\left\{\xi_1^* \quad \xi_2^* \quad \xi_3^*\right\} \tag{7}$$

where ξ is the determinant of the matrix $[C]^{ic}$ and ξ_i^*, $i = 1, 2, 3$, are the determinants of the matrices obtained by replacing the ith column with right-hand side of Eq. (6). M and M^* are the minors of the corresponding matrices:

$$\xi = \sum_{j=1}^{3}(-1)^{j+k}C_{jk}M_{jk}, \qquad k = 1, 2, \text{or } 3$$

$$\xi_k^* = \sum_{j=1}^{3}(-1)^{j+k}\left(\sigma_j + e_{3j}E_Z^P\right)M_{jk}^*, \qquad k = 1, 2, \text{or } 3$$

It is assumed in the shear lag model that the difference in the normal displacements in fiber and matrix is proportional to the shear stress at the matrix–fiber interface, that is,

$$\left\{\frac{\partial\sigma}{\partial x}\right\}^{\text{ic}} = -\{c\tau\} = [H](\{u\}^{\text{ic}} - \{u\}^{m}) \tag{8}$$

where

$$\left\{\frac{\partial\sigma}{\partial x}\right\}^{\text{ic}} = \left\{\frac{\partial\sigma_x}{\partial x} \quad \frac{\partial\sigma_y}{\partial y} \quad \frac{\partial\sigma_z}{\partial z}\right\}^{\text{ic}}$$

$$\{c\tau\}^{\text{ic}} = \left\{\frac{2(b^{\text{ic}}+t^{\text{ic}})}{b^{\text{ic}}t^{\text{ic}}}\tau_1 \quad \frac{2(\ell^{\text{ic}}+t^{\text{ic}})}{\ell^{\text{ic}}t^{\text{ic}}}\tau_2 \quad \frac{2(b^{\text{ic}}+\ell^{\text{ic}})}{b^{\text{ic}}\ell^{\text{ic}}}\tau_3\right\}^{\text{ic}}$$

$$[H] = \begin{bmatrix} h_1 & 0 & 0 \\ 0 & h_2 & 0 \\ 0 & 0 & h_3 \end{bmatrix}, \qquad \{U\}^{\text{ic}} = \{u \quad v \quad w\}^{\text{ic}}$$

$$\{U\}^{m} = \{u \quad v \quad w\}^{m}$$

The first equation of Eq. (7) is obtained by considering the equilibrium of forces along the x, y, and z directions, respectively. Note that the positive direction of shear stress is taken along the positive direction of the coordinate axes.

The constants given in $[H]$ will be determined in Appendix A. When the second equation given in Eq. (7) is differentiated with respect to x, y, and z, and relation (8) is used, the following relation is obtained:

$$\left\{\frac{\partial^2\sigma}{\partial x^2}\right\}^{\text{ic}} = [H]\left(\left\{\frac{\partial u}{\partial x}\right\}^{\text{ic}} - \{s\}\right) \tag{9}$$

From Fig. 2 it can be clearly estimated that the strain in matrix medium is equal to the applied strain in the composite, that is,

$$\left\{\frac{\partial U}{\partial x}\right\}^{m} = \{s\} = \{s_x \quad s_y \quad s_z\} \tag{10}$$

When Eqs. (7) and (9) are used, the following expression is obtained:

$$\left\{\frac{\partial^2\sigma}{\partial x^2}\right\}^{\text{ic}} = \frac{1}{\xi}[H]\left(\{\sigma\}^{\text{ic}^T} + \{e\}^{\text{ic}^T}\boldsymbol{E}_z^{\text{ic}}\right)(\{C^{f^*}\} - \xi\{s\}) \tag{11}$$

where $\{C^{f^*}\}$ is vector of the cofactors obtained by replacing the i th column of matrix $[C]^{\text{ic}}$ with right-hand side of Eq. (6).

The general solution of Eq. (11) can be represented as (Appendix B)

$$[G]^1\{\sigma\}^{\text{ic}} = [G]^2\{s\} + \{G\}^3\boldsymbol{E}_z^{\text{ic}} \tag{12}$$

where

$$G_{ij}^1 = \begin{cases} \left(C_{ij}^{f^*}/C_{ii}^{f^*}\right)\left[1 + \left(2/\beta_i\ell^c\right)\left(\sigma_{x_i}^0/\sigma_{x_i}^{\text{ic}}\right)\right. \\ \qquad \left.\times \tan\text{h}\left(\beta_i\ell^c/2\right)\right], & i \neq j \\ 1, & i = j \end{cases}$$

$$G_{ij}^2 = \begin{cases} \left(\xi/C_{ii}^{f^*}\right)\left[1 + \left(2/\beta_i\ell^c\right)\tan\text{h}(\beta_i\ell_c/2)\right] \\ \qquad + \left(2/\beta_i\ell^c\right)\left(\sigma_{x_i}^0/s_{x_i}\right), & i = j \\ 0, & i \neq j \end{cases}$$

$$G_i^3 = \left[1 + \left(2/\beta_i\ell^c\right)\tan\text{h}\left(\beta_i\ell^c/2\right)\right]\left[e_{31}^{\text{ic}} + \left(C_{2i}^{f^*}/C_{ii}^{f^*}\right)e_{32}^{\text{ic}} + \left(C_{3i}^{f^*}/C_{ii}^{f^*}\right)e_{33}^{\text{ic}}\right]$$

The composite stresses can be obtained from the individual component stresses by using the rule of mixture, that is,

$$\{\sigma\}^c = [f]^{\text{ic}}\{\sigma\}^{\text{ic}} + [f]^m\{\sigma\}^m \tag{13}$$

In which $[f]^{\text{ic}}$ and $[f]^m$ are volume fraction matrices of inclusion and matrix and $[f]^{\text{ic}} + [f]^m = I$ of appropriate dimension. These two matrices can be chosen according to a particular situation.

When Eqs. (12) and (13) are used and compared with the constitutive relation of the composite, effective properties of the composite can be determined:

$$\{\sigma\}^c = \left([f]^{\text{ic}}[G]^{1^{-1}}[G]^2 + [f]^m[C]^m\right)\{s\} + \left([f]^{\text{ic}}[G]^{1^{-1}}\{G\}^3\boldsymbol{E}_z^{\text{ic}} - [f]^m[e]^m\boldsymbol{E}_z^m\right) \tag{14}$$

The effective stiffness properties of the composite $[C]^c$ can be obtained from Eq. (14) and are given by

$$[C]^c = [f]^{\text{ic}}[G]^{1^{-1}}[G]^2 + [f]^m[C]^m \tag{15}$$

To obtain the effective piezoelectric properties of the composite, the relation of electric fields in both the constituent mediums must be established. If the electric field is so applied that they are the same in both inclusion and matrix and equal to the composite applied field, then the effective piezoelectric properties are given by

$$\{e\}^c = [f]^{\text{ic}}[G]^{1^{-1}}\{G\}^3 - [f]^m\{e\}^m \tag{16}$$

For piezoelectric inclusion in a matrix medium that is piezoelectrically inactive, for an isoelectric field case, the effective properties are obtained as

$$\{e\}^c = [f]^{\text{ic}}[G]^{1^{-1}}\{G\}^3 \tag{17}$$

For matrix inclusion inside a piezoelectric medium, $\{G\}^3$ is a null vector, and for the isoelectric field case, the effective properties can be given as

$$\{e\}^c = -[f]^m\{e\}^m \tag{18}$$

If electric field is applied so that they are not the same in both the inclusion and matrix and the effective composite electric field can be represented by rule of mixture, then the effective piezoelectric properties are given by

$$\{e\}^c = [G]^{1^{-1}}\{G\}^3\boldsymbol{E}_z^c - [f]^m\left([G]^{1^{-1}}\{G\}^3 + \{e\}^m\right)\boldsymbol{E}_z^m \tag{19}$$

In this case, another relation is required to determine the effective piezoelectric properties of the composite. There is another requirement that dielectric displacement along the z direction should be same in both of the constituent mediums to ensure compatibility of displacements. This condition can be represented by the following relation:

$$\varepsilon_{33}^m\boldsymbol{E}_z^m - \varepsilon_{33}^{\text{ic}}\boldsymbol{E}_z^{\text{ic}} = \left(\{e\}^{\text{ic}^T} - \{e\}^{m^T}\right)\{s\} \tag{20}$$

By the use of the rule of mixture for an electric field, in Eq. (20), $\boldsymbol{E}_z^m$ can be represented in terms of $\boldsymbol{E}_z^c$ and $\{s\}$ as follows:

$$\boldsymbol{E}_z^m = \frac{\varepsilon_{33}^{\text{ic}}}{f^m\varepsilon_{33}^{\text{ic}} + f^{\text{ic}}\varepsilon_{33}^m}\boldsymbol{E}_z^c - \frac{f^{\text{ic}}\varepsilon_{33}^{\text{ic}}}{\varepsilon_{33}^m}\left(\{e\}^{\text{ic}^T} - \{e\}^{m^T}\right)\{s\} \tag{21}$$

When Eqs. (14) and (21) and the rule of mixture are used, effective piezoelectric properties of the composite for the case when electric fields are not same in constituent mediums are obtained as

$$\{e\}^c = \frac{f^{\text{ic}}\varepsilon_{33}^m}{f^m\varepsilon_{33}^{\text{ic}} + f^{\text{ic}}\varepsilon_{33}^m}[G]^{1^{-1}}\{G\}^3 - \frac{f^m\varepsilon_{33}^{\text{ic}}}{f^m\varepsilon_{33}^{\text{ic}} + f^{\text{ic}}\varepsilon_{33}^m}\{e\}^m \tag{22}$$

For piezoelectric inclusion in a matrix medium that is piezoelectrically inactive, for the nonisoelectric field case, effective properties are obtained as

$$\{e\}^c = \frac{f^{\text{ic}}\varepsilon_{33}^m}{f^m\varepsilon_{33}^{\text{ic}} + f^{\text{ic}}\varepsilon_{33}^m}[G]^{1^{-1}}\{G\}^3 \tag{23}$$

For piezoelectrically inactive matrix inclusion inside a piezoelectric medium, $\{G\}^3$ is a null vector, and for the nonisoelectric field case, the effective properties can be given as

$$\{e\}^c = -\frac{f^{\text{ic}}\varepsilon_{33}^m}{f^m\varepsilon_{33}^{\text{ic}} + f^{\text{ic}}\varepsilon_{33}^m}\{e\}^m \tag{24}$$

III. Numerical Examples

The numerical values of the effective properties of the piezoelectric composites are evaluated using the method discussed in the preceding section. The material properties of the piezoelectric medium and matrix medium considered are listed in Table 1. First the method described in the preceding section is verified by using the inclusion as long fiber equal in length to the composite. Figure 3 shows the variation of the effective stiffness coefficient C_{11} with fiber volume fraction. Figure 3 shows the results obtained from shear lag model derived in the preceding section and compares it with the method of cells and strength of materials approaches derived by Mallik and Ray.[5] The variation of ratio $e31r$ with fiber volume fraction is shown in Fig. 4. The ratio $e31r$ is defined as $e_{31}^c/e_{31}^{\text{ic}}$. Figure 4 also shows a comparison of the three methods, namely, shear lag model, method of cells, and strength of materials. From Figs. 3 and 4, it can be concluded that the shear lag model provides prediction of effective properties of PFRC that closely follows the predictions made by Mallik and Ray[5] with the help of the method of cells and strength of materials approaches. Thus, the present model is validated. It can be observed from Fig. 4 that effective piezoelectric properties in the longitudinal direction when electric field is applied transversely improve beyond a certain fiber volume fraction. Figures 5–12 present the effective properties of the short piezoelectric fiber composite obtained by the shear lag method. In Figs. 5–7, the width and thickness dimensions are kept constant and length dimension is varied to find its effect on effective stiffness property (Fig. 5) and effective piezoelectric property for the isoelectric field (Fig. 6) and nonisoelectric field (Fig. 7). Figures 5–7 show that as width and thickness dimensions decrease the effective stiffness

Table 1 Material properties

Property	PZT5H	Epoxy
C_{11}, GPa	151	3.86
C_{12}, GPa	98	2.57
C_{13}, GPa	96	2.57
C_{33}, GPa	124	3.86
e_{31}, C/m^2	−5.1	0
e_{32}, C/m^2	−5.1	0
e_{33}, C/m^2	27	0
ε_{33}, 10^{-9} C/V·m	13.27	0.079

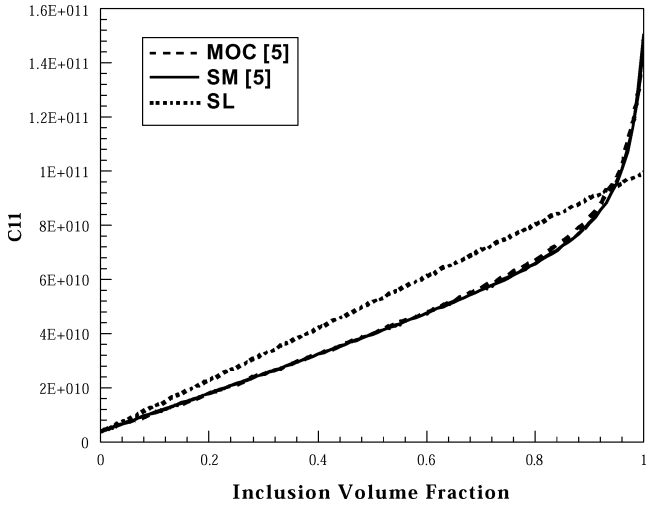

Fig. 3 Comparison of effective stiffness properties by three methods.

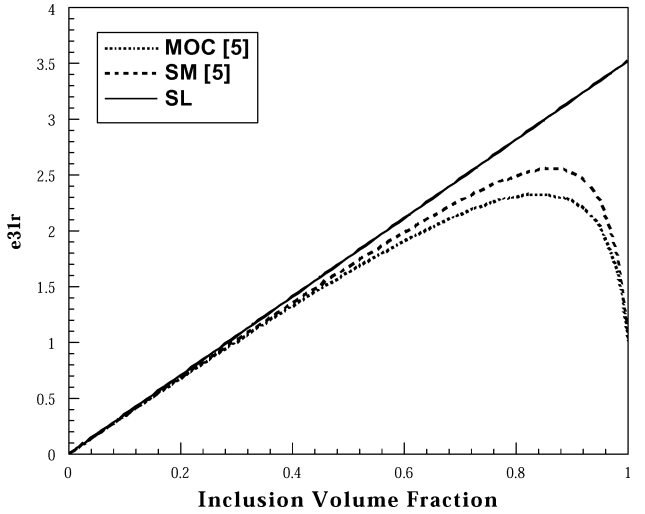

Fig. 4 Comparison of effective piezoelectric property by three methods.

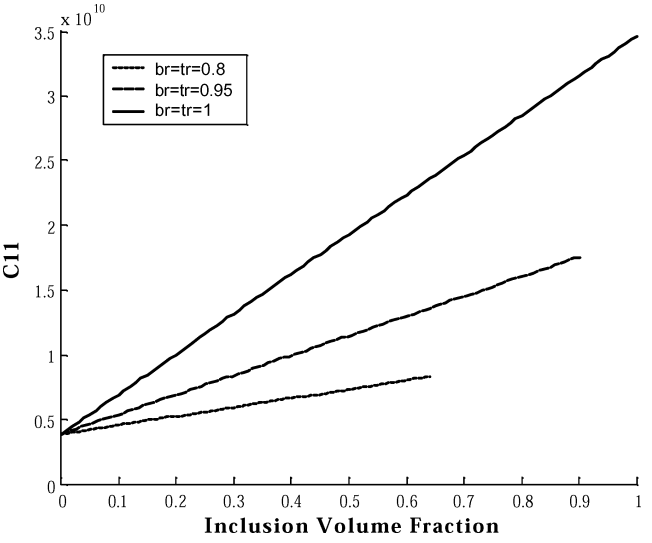

Fig. 5 Effect of inclusion geometry on effective stiffness property.

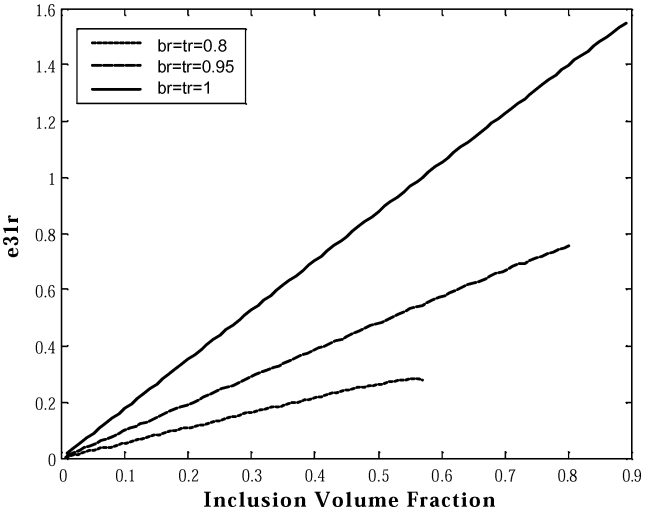

Fig. 6 Effect of inclusion geometry on effective piezoelectric property with isoelectric field.

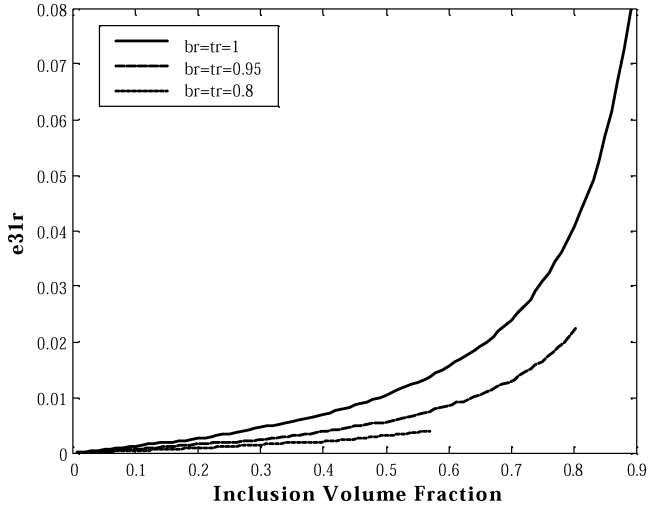

Fig. 7 Effect of inclusion geometry on effective piezoelectric property with nonisoelectric field.

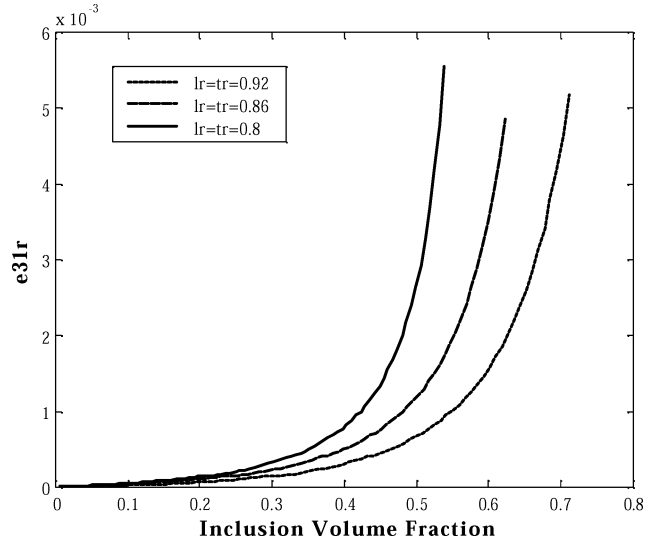

Fig. 8 Effect of inclusion geometry on effective piezoelectric property with isoelectric field.

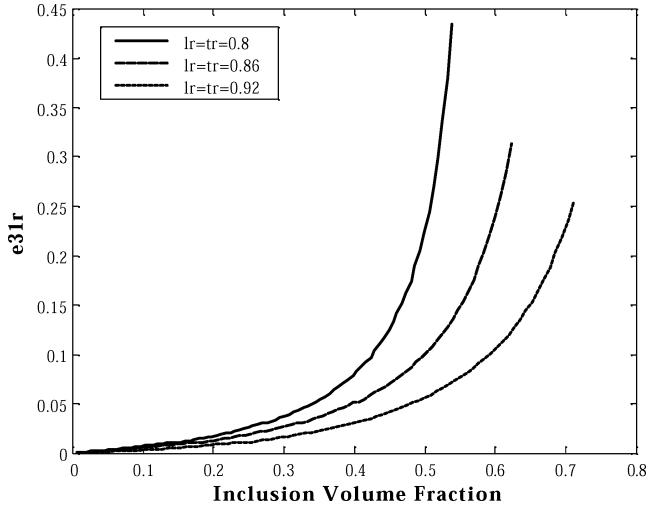

Fig. 9 Effect of inclusion geometry on effective piezoelectric property with nonisoelectric field.

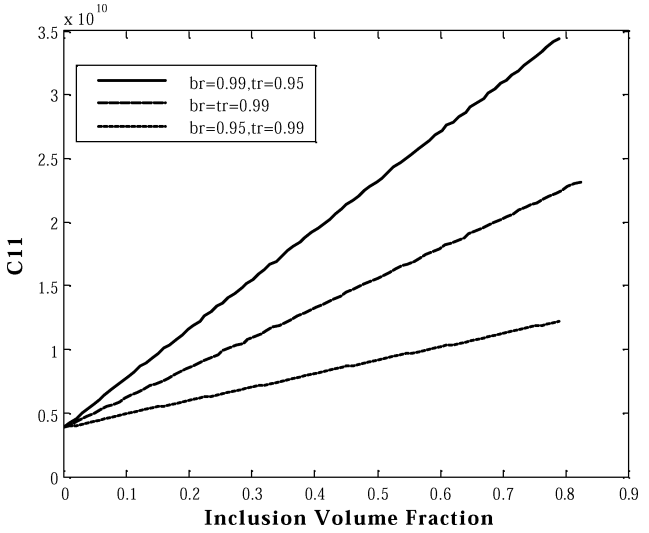

Fig. 10 Effect of shape of inclusion on effective stiffness property.

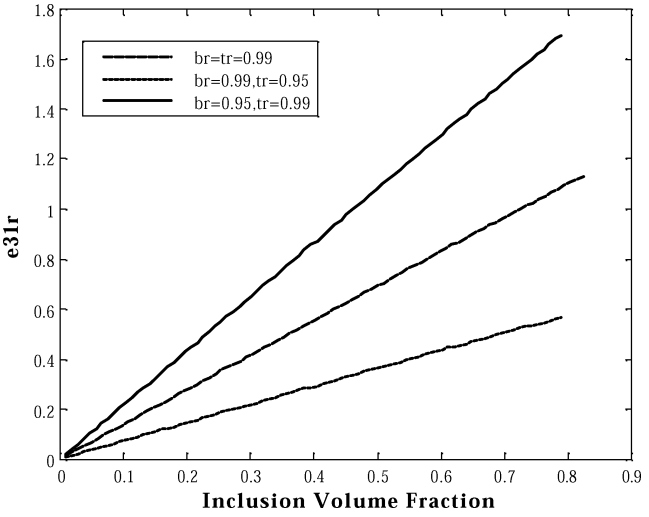

Fig. 11 Effect of shape of inclusion on effective piezoelectric property with isoelectric field.

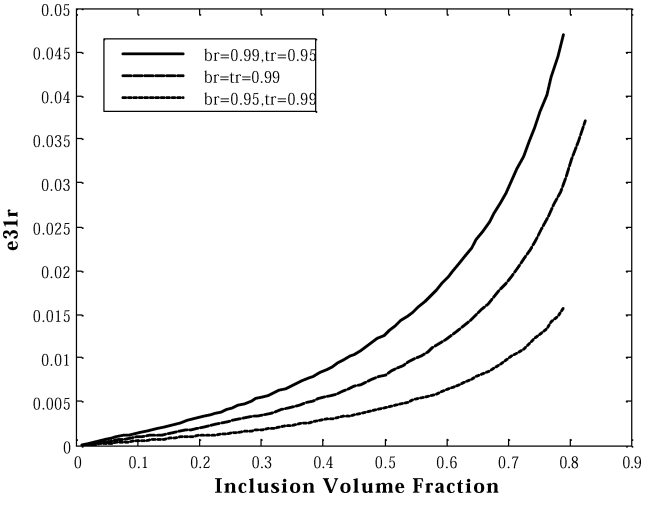

Fig. 12 Effect of shape of inclusion on effective piezoelectric property with nonisoelectric field.

property C_{11}^{c} and effective piezoelectric property, $e_{31}^{r} = e_{31}^{c}/e_{31}^{\text{ic}}$, for both of the cases of electric fields decrease. Figures 5–7 also predict that as the length dimension of the piezoelectric inclusion decreases the effective properties decrease. Figures 5–7 provide a quantitative measure of the effective properties of piezoelectric inclusion. Figures 6 and 7 clearly demonstrate that the isoelectric field predicts a better effective piezoelectric property than the nonisoelectric field for the same inclusion geometry. The effect of the variation of the width dimension by keeping the length and thickness dimensions of the inclusion on the effective piezoelectric properties is presented in Figs. 8 and 9. Figures 8 and 9 show that as length and thickness decrease the effective piezoelectric property increases for both cases of electric fields. It is also observed from Figs. 8 and 9 that the effective piezoelectric property decreases with a decrease in width dimension. Figures 10–12 show the variation of effective properties with the shape of the transverse cross section of the inclusion. The effective stiffness of the composite decreases when the thickness is decreased more than width and increases when thickness is increased more than width over that of when cross section is square as shown in Fig. 10. The response reverses for the case of greater width than thickness. It is observed from the Figs 11 and 12 that the effect on the effective piezoelectric property for the cases of iso- and nonisoelectric fields is same as that of the effective stiffness property when the shape of the transverse cross section is varied from square. Similarly, all of the other effective properties are obtained from this analysis but are not shown here.

IV. Conclusions

The methodology for determining the effective mechanical and piezoelectric properties of piezoelectric composites having piezoelectric short fibers as inclusions discussed. Both homogeneous and heterogeneous inclusions are treated. The inclusion considered in this study is that of a rectangular parallelepiped type. Both isoelectric fields and nonisoelectric fields are considered. The effect of shape and size of inclusion on the effective stiffness and piezoelectric properties is studied. It observed that effective stiffness and piezoelectric properties are strongly dependent on the shape and size of the inclusion. It is also observed that for a particular size of inclusion, the effective piezoelectric property improves over that of a monolithic material. Study of other kind of inclusions, such as circular or elliptical, is beyond the scope of this study. Experimental investigation is an obvious choice for verification of results. Also, other theoretical methods can be applied for verification of results.

Appendix A: Evaluation of Constant Matrix *H*

To find the constants h_i, the following procedure is used. Force equilibrium at arbitrary point ($z = z$) and at $z = t_f/2$ provides

$$2b^{c}\tau_1^{m} = 2b^{\text{ic}}\boldsymbol{\tau}_1^{\text{interface}} \tag{A1}$$

The shear strain γ at any arbitrary point $z = z$ is related to $\boldsymbol{\tau}_1^{m}$ as

$$\gamma = \frac{\mathrm{d}u^{m}}{\mathrm{d}z} = \frac{\boldsymbol{\tau}_1^{m}}{C_{44}^{m}} = \frac{b^{\text{ic}}\boldsymbol{\tau}_1^{\text{interface}}}{b^{c}C_{44}^{m}} \tag{A2}$$

where $\boldsymbol{\tau}^{m}$ is the shear stress in the matrix at any point $z = z$ and C_{44}^{m} is the shear modulus of the matrix. When Eq. (A2) is integrated from $z = w^{\text{ic}}/2$ to $z = w^{c}/2$, the following relation is obtained:

$$u^{m} - u^{\text{ic}} = \frac{b^{r}(b^{c} - b^{\text{ic}})\boldsymbol{\tau}_1^{\text{interface}}}{2C_{44}^{m}} \tag{A3}$$

where $b^{r} = b^{\text{ic}}/b^{c}$.

Similarly, force equilibrium at arbitrary point ($y = y$) and at $y = b^{\text{ic}}/2$ provides

$$2t^{\text{ic}}\boldsymbol{\tau}_2^{m} = 2t^{\text{ic}}\boldsymbol{\tau}_1^{\text{interface}} \tag{A4}$$

The shear strain γ at any arbitrary point $y = y$ is related to $\boldsymbol{\tau}_2^{m}$ as

$$\gamma = \frac{\mathrm{d}u^{m}}{\mathrm{d}y} = \frac{\boldsymbol{\tau}_2^{m}}{C_{44}^{m}} = \frac{\boldsymbol{\tau}_1^{\text{interface}}}{C_{44}^{m}} \tag{A5}$$

where $\boldsymbol{\tau}_2^{m}$ is the shear stress in the matrix at any point $y = y$ and C_{44}^{m} is the shear modulus of the matrix. When Eq. (A2) is integrated from $y = t^{\text{ic}}/2$ to $y = t^{c}/2$, the following relation is obtained:

$$u^{m} - u^{\text{ic}} = \frac{(t^{c} - t^{\text{ic}})\boldsymbol{\tau}_1^{\text{interface}}}{2C_{44}^{m}} \tag{A6}$$

Thus, the total difference in axial displacement between the matrix and fiber is the sum of Eqs. (A3) and (A6). When compared with Eq. (8), constant h_1 is obtained as

$$h_1 = \frac{4C_{44}^{m}(b^{\text{ic}} + t^{\text{ic}})}{b^{\text{ic}}t^{\text{ic}}\{b^{r}(b^{c} - b^{\text{ic}}) + (t^{c} - t^{\text{ic}})\}} \tag{A7}$$

In a similar fashion, constants h_2 and h_3 are obtained as

$$h_2 = \frac{4C_{44}^{m}(\ell^{\text{ic}} + t^{\text{ic}})}{\ell^{\text{ic}}t^{\text{ic}}\{\ell^{r}(\ell^{c} - \ell^{\text{ic}}) + (t^{c} - t^{\text{ic}})\}} \tag{A8}$$

$$h_3 = \frac{4C_{44}^{m}(\ell^{\text{ic}} + b^{\text{ic}})}{\ell^{\text{ic}}b^{\text{ic}}\{\ell^{r}(\ell^{c} - \ell^{\text{ic}}) + (b^{c} - b^{\text{ic}})\}} \tag{A9}$$

Appendix B: Solution of Differential Equation Given in Eq. (11)

From Eq. (11), the following relation is obtained:

$$\frac{\partial^2\sigma_x^{\text{ic}}}{\partial x^2} = \frac{h_1}{\xi/M_{11}^{*}}\left[\sigma_x^{\text{ic}} - \frac{M_{12}^{*}}{M_{11}^{*}}\sigma_y^{\text{ic}} + \frac{M_{13}^{*}}{M_{11}^{*}}\sigma_z^{\text{ic}} + \left(e_{31}^{\text{ic}} - \frac{M_{12}^{*}}{M_{11}^{*}}e_{32}^{\text{ic}} + \frac{M_{13}^{*}}{M_{11}^{*}}e_{33}^{\text{ic}}\right)\boldsymbol{E}_z^{\text{ic}} - \frac{\xi}{M_{11}^{*}}s_x\right] \tag{B1}$$

The general solution to Eq. (B1) is given by

$$\sigma_x^{\text{ic}} = \left(\xi/M_{11}^{*}\right)s_x - \left(M_{12}^{*}/M_{11}^{*}\right)\sigma_y^{\text{ic}} + \left(M_{13}^{*}/M_{11}^{*}\right)\sigma_z^{\text{ic}} + \left[e_{31}^{\text{ic}} - \left(M_{12}^{*}/M_{11}^{*}\right)e_{32}^{\text{ic}} + \left(M_{13}^{*}/M_{11}^{*}\right)e_{33}^{\text{ic}}\right] \times \boldsymbol{E}_z^{\text{ic}} + c_1\cos\mathrm{h}\beta_1 x + c_2\sin\mathrm{h}\beta_1 x \tag{B2}$$

where $\beta_1 = \sqrt{[h_1/(\xi/M_{11}^{*})]}$ and c_1 and c_2 are the unknown constants. These unknown constants can be determined from boundary conditions. The boundary conditions are

$$\frac{\partial\sigma_x^{\text{ic}}}{\partial x} = 0 \qquad \text{at} \qquad x = 0 \tag{B3}$$

$$\sigma_x^{\text{ic}} = \sigma_x^{0}, \qquad \sigma_y^{\text{ic}} = \sigma_y^{0}, \qquad \sigma_z^{iz} = \sigma_z^{0} \qquad \text{at} \qquad x = \frac{\ell^{\text{ic}}}{2} \tag{B4}$$

With the help of the Eqs. (33–35), the following relation for the axial stress in piezoelectric fiber medium can be obtained as

$$\sigma_x^{\text{ic}} = \frac{\xi}{M_{11}^{*}}s_x - \frac{M_{12}^{*}}{M_{11}^{*}}\sigma_y^{\text{ic}} + \frac{M_{13}^{*}}{M_{11}^{*}}\sigma_z^{\text{ic}} + \left(e_{31}^{\text{ic}} - \frac{M_{12}^{*}}{M_{11}^{*}}e_{32}^{\text{ic}} + \frac{M_{13}^{*}}{M_{11}^{*}}e_{33}^{\text{ic}}\right) \times \boldsymbol{E}_z^{\text{ic}} + \left\{\left[\sigma_x^{0} - \frac{\xi}{M_{11}^{*}}s_x - \frac{M_{12}^{*}}{M_{11}^{*}}\sigma_y^{0} + \frac{M_{13}^{*}}{M_{11}^{*}}\sigma_z^{0} + \left(e_{31}^{\text{ic}} - \frac{M_{12}^{*}}{M_{11}^{*}}e_{32}^{\text{ic}} + \frac{M_{13}^{*}}{M_{11}^{*}}e_{33}^{\text{ic}}\right)\boldsymbol{E}_z^{\text{ic}}\right]\Big/\cos\mathrm{h}\left(\beta_1\ell^{\text{ic}}/2\right)\right\}\cos\mathrm{h}\beta_1 x \tag{B5}$$

The average fiber stress $\bar{\sigma}_x^{\text{ic}}$ is computed as follows:

$$\bar{\sigma}_x^{\text{ic}} = \frac{2}{\ell^{c}}\int_0^{\ell^{c}/2}\sigma_x^{\text{ic}}\,\mathrm{d}x \tag{B6}$$

When Eqs. (B5) and (B6) are used and rearranging, the average axial stress $\bar{\sigma}_x^{\text{ic}}$ in fiber can be expressed as follows:

$$\bar{\sigma}_x^{\text{ic}} = g_1\epsilon + g_2\sigma_y^{\text{ic}} + g_3\sigma_z^{\text{ic}} + g_4\boldsymbol{E}_z^{\text{ic}} \tag{B7}$$

where

$$g_1 = \xi / M_{11}^* + \left(2/\beta_1 \ell^c\right)\left(\sigma_x^0 / s_x - \xi / M_{11}^*\right) \tanh\left(\beta_1 \ell^c / 2\right)$$

$$g_2 = \left(M_{12}^* / M_{11}^*\right)\left[1 - \left(2/\beta_1 \ell^c\right)\left(\sigma_y^0 / \sigma_y^{\text{ic}}\right) \tanh\left(\beta_1 \ell^c / 2\right)\right]$$

$$g_3 = \left(M_{13}^* / M_{11}^*\right)\left[\left(2/\beta_1 \ell^c\right)\left(\sigma_z^0 / \sigma_z^{\text{ic}}\right) \tanh\left(\beta_1 \ell^c / 2\right) - 1\right]$$

$$g_4 = \left[e_{31}^{\text{ic}} - \left(M_{12}^* / M_{11}^*\right) e_{32}^{\text{ic}} + \left(M_{13}^* / M_{11}^*\right) e_{33}^{\text{ic}}\right] \times \left[1 - \left(2/\beta_1 \ell^c\right) \tanh\left(\beta_1 \ell^c / 2\right)\right] \tag{B8}$$

In a similar manner from the other two equations, from Eq. (11) all other constants of Eq. (16) can be obtained.

References

[1]Aboudi, J., "Micromechanical Prediction of the Effective Coefficients of Thermo-Piezoelectric Multiphase Composites," *Journal of Intelligent Material Systems and Structures*, Vol. 9, 1998, pp. 713–722.

[2]Smith, W. A., and Auld, B. A., "Modelling 1-3 Composite Piezoelectrics: Thickness Mode Oscillations," *IEEE Transactions on Ultrasonics, Ferroelectrics and Frequency Control*, Vol. 40, 1991, pp. 40–47.

[3]Dunn, M. L., and Taya, M., "Micromechanics Predictions of the Effective Electroelastic Moduli of Piezoelectric Composites," *International Journal of Solids and Structures*, Vol. 30, 1993, pp. 161–175.

[4]Mallik, N., and Ray, M. C., "Effective Coefficients of Piezoelectric Fiber-Reinforced Composites," *AIAA Journal*, Vol. 41, No. 4, 2003, pp. 704–710.

[5]Mallik, N., "Effective Properties of Piezoelectric Composites in Plane Stress," *AIAA Journal* (submitted for publication).

[6]Eshelby, J. D., "The Determination of the Elastic Field of an Ellipsoidal Inclusion, and Related Problems," *Proceedings of the Royal Society of London*, Vol. A241, 1957, pp. 376–396.

[7]Cox, H. L., *Journal of Applied Physics*, Vol. 3, 1952, p. 72.

[8]Kelly, A., *Strong Solids*, 2nd ed., Oxford Univ. Press, 1973, Chap. 5.

[9]Taya, M., and Arsenault, R. J., *Metal Matrix Composites: Thermomechanical Behavior*, Pergamon, New York, 1989, Chaps. 1 and 2.

[10]Mura, T., *Mechanics of Elastic and Inelastic Solids 3: Micromechanics of Defects in Solids*, Martinus Nijhoff, The Hague, The Netherlands, 1982, Chap. 1.

[11]Huang, J. H., "Equivalent Inclusion Method for the Work-Hardening Behavior of Piezoelectric Composites," *International Journal of Solids and Structures*, Vol. 33, No. 10, 1996, pp. 1439–1451.

[12]Chan, H. L. W., and Unsworth, J., "Simple Model for Piezoelectric Ceramic/Polymer 1-3 Composites Used in Ultrasonic Transducer Applications," *IEEE Transactions on Ultrasonics, Ferroelectrics and Frequency Control*, Vol. 36, No. 4, 1989, pp. 434–441.

[13]Hossack, J. A., and Hayward, G., "Finite Element Analysis of 1-3 Composite Transducers," *IEEE Transactions on Ultrasonics, Ferroelectrics and Frequency Control*, Vol. 38, No. 6, 1991, pp. 618–629.

[14]Chen, T., "Effective Properties of Platelet Reinforced Piezocomposites," *Composites: Part B*, Vol. 27B, 1996, pp. 467–474.

[15]Yuan, F. G., Pagano, N. J., and Cai, X., "Elastic Moduli of Brittle Matrix Composites with Interfacial Debonding," *International Journal of Solids and Structures*, Vol. 34, No. 2, 1997, pp. 177–201.

[16]Tiersten, H. F., *Linear Piezoelectric Plate Vibrations*, Plenum, New York, 1969, Chaps. 1 and 2.

A. Palazotto
Associate Editor